ELSEVIER
Journal of Nuclear Materials 290–293 (2001) 299–302
journal of nuclear materials
www.elsevier.nl/locate/jnucmat

Effects of condensible impurities on the erosion behavior of the plasma-facing materials

N. Ohno [a,*], S. Uno [a], Y. Hirooka [b], S. Takamura [a]

[a] *Department of Energy Engineering and Science, Graduate School of Engineering, Nagoya University, Furo-cho Chikusa-ku, Nagoya 464-8603, Japan*
[b] *National Institute for Fusion Science, Toki, Gifu 509-5292, Japan*

Abstract

Effects of condensible plasma impurities on the material erosion behaviors have been investigated by improving the previous zero-dimensional model. The new model can describe more precisely the transition from the enhanced erosion due to impurities to reduced erosion with the formation of the impurity film. Model predictions have been proven by the experimental observations in NAGDIS-I. A water-cooled molybdenum target plate was bombarded with argon plasmas into which methane was introduced as carbon impurity. As the flow rate of the methane gas was increased, MoI emission line intensity, corresponding to sputtered particle flux, has been observed to decrease to a great deal. © 2001 Published by Elsevier Science B.V.

Keywords: Carbon deposition; Plasma facing materials; Condensible impurity; Carbon; Erosion; Sputtering

1. Introduction

The control of impurity generation has been one of the most critical subjects in the fusion research [1–3]. In the next generation fusion devices intended to have steady-state operation, high Z materials such as tungsten are thought to be candidates for the divertor plate. It is, however, well known that the contamination of high Z materials strongly deteriorates the performance of the core plasma. It is necessary to develop a method for suppressing the impurity emission. The recent systematic analysis on effects of plasma impurities on the erosion behavior of plasma-facing materials based on zero-dimensional materials balance modeling [1,2] has predicted that condensible impurities such as carbon can form an impurity film, resulting in a significant reduction or even complete elimination of the host materials erosion.

In this report, we present the data taken in NAGDIS-I demonstrating reduced erosion of the host material erosion. Also, we have improved the zero-dimensional model and applied the improved model for the data analysis.

2. Modeling for erosion behaviors with condensible impurity

The zero-dimensional mass balance model [1] predicts two completely different effects of carbon impurity; enhanced erosion due to the physical sputtering and suppressed erosion of the plasma-facing material by the deposited carbon films. Molybdenum is assumed to be a plasma-facing material. The numerical result by using the mass balance model in [1] is shown as a thick dashed line in Fig. 1(a). The rapid change between two conditions occurs at $R = R_c$, at which the Mo surface is fully covered with carbon impurities, where R is the flux ratio of carbon impurity to host plasma species to the target, because it is assumed that there is no deposited carbon on the Mo surface until the surface is fully covered with

---

[*] Corresponding author. Tel.: +81-52 789 3145; fax: +81-52 789 3944.
E-mail address: ohno@ees.nagoya-u.ac.jp (N. Ohno).

0022-3115/01/$ - see front matter © 2001 Published by Elsevier Science B.V.
PII: S0022-3115(00)00631-0

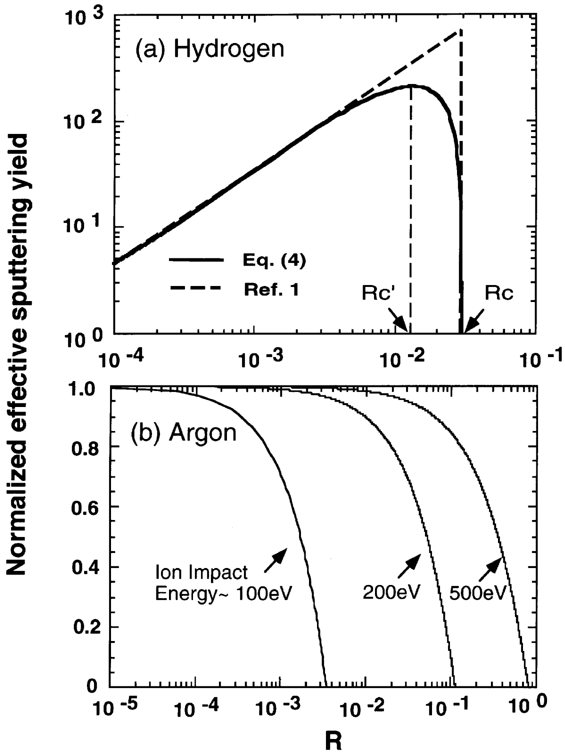

Fig. 1. Dependence of normalized effective sputtering yields on the ratio of: (a) the carbon ion flux to hydrogen ion flux to the target plate, R. Dashed line is data in [1] and solid line calculated from Eq. (4). $\sigma_{H^+\to Mo}$, $\sigma_{C^+\to Mo}$ and $\sigma_{C^+\to C}$ are 2.5×10^{-25}, 8.5×10^{-21}, and 9.4×10^{-21} (m^2), where the incident ion energy is assumed to be 300 eV; (b) the carbon ion flux to argon ion flux as a parameter of the incident ion energy.

the carbon atoms. Unfortunately, this model is not capable of describing the transition of erosion behavior.

In this section, details of the improvement on the zero-dimensional mass balance model will be described. Here, we use the concept of cross-section for sputtering [4], so that the sputtering yield can be treated as a function of surface coverage.

The surface concentration of deposited carbon on the host material, $C_s(t)$ (m^{-2}), can be expressed by the following manner:

$$\frac{dC_s(t)}{dt} = -\Gamma_{A^+}\sigma_{A^+\to C}C_s(t) - \Gamma_{C^+}\sigma_{C^+\to C}C_s(t) + \Gamma_{C^+}v, \tag{1}$$

where the subscript ‘A’ means the host plasma species such as H, He and Ar, which are usually used for plasma production in our experimental device. Γ_{A^+} is the flux of host plasma species to the material surface, Γ_{C^+} the carbon impurity flux, and $\sigma_{A^+\to C}$, $\sigma_{C^+\to C}$ the sputtering cross-sections of carbon bombarded by host plasma ions and carbon ions and v is the deposition rate of carbon on molybdenum. Eq. (1) can be solved under the initial condition $C_s = 0$ at $t = 0$. The solution is

$$C_s(t) = \frac{Rv}{\sigma_{A^+\to C} + R\sigma_{C^+\to C}} \times \{1 - \exp(-\Gamma_{A^+}(\sigma_{A^+\to C} + R\sigma_{C^+\to C})t)\}, \tag{2}$$

where $R = \Gamma_{C^+}/\Gamma_{A^+}$. Eq. (2) shows the coverage over molybdenum with carbon. The steady-state surface coverage $C_s(\infty)$ is given by $Rv/(\sigma_{A^+\to C} + R\sigma_{C^+\to C})$. On the other hand, the molybdenum particle flux, Γ_{Mo}, from the target plate due to physical sputtering is expressed by

$$\Gamma_{Mo}(t) = \Gamma_{A^+}(\sigma_{A^+\to Mo} + R\sigma_{C^+\to Mo})\left\{1 - \frac{C_s(t)}{C_{s0}}\right\}M_{s0}, \tag{3}$$

where C_{s0} and M_{s0} are the surface concentration of pure carbon and molybdenum, respectively. Finally, the effective sputtering yield Y_{eff} defined by $\Gamma_{Mo}(\infty)/\Gamma_{A^+}$ is written to be

$$\frac{Y_{eff}(R)}{Y_{A^+\to Mo}} = \left(1 + R\frac{Y_{C^+\to Mo}}{Y_{A^+\to Mo}}\right) \times \left(1 - \frac{Rv}{Y_{A^+\to C} + RY_{C^+\to C}}\right), \tag{4}$$

where $Y_{A^+\to Mo} = \sigma_{A^+\to Mo}M_{s0}$, $Y_{C^+\to Mo} = \sigma_{C^+\to Mo}M_{s0}$, $Y_{A^+\to C} = \sigma_{A^+\to C}C_{s0}$ and $Y_{C^+\to C} = \sigma_{C^+\to C}C_{s0}$ [5,6]. The first bracket in the right-hand side represents the erosion enhancement due to the carbon impurities and the second bracket means the suppression of the erosion rate due to the surface coverage with the deposited carbon.

Fig. 1 shows the dependence of normalized effective sputtering yield $Y_{eff}(R)/Y_{A^+\to Mo}$ on the flux ratio of carbon impurity to host plasma to the target, R, calculated from Eq. (4). In Fig. 1(a), hydrogen plasma is assumed to be the host plasma and the incident energy of carbon and hydrogen ions is 300 eV. When the flux ratio of carbon impurity to hydrogen plasma is small, the normalized effective sputtering yield is increasing with$R$. On further increasing R, the dashed line gives the breaking point at the critical ratio, R_c, at which molybdenum is fully covered with carbon as mentioned before. Then the critical ratio, R_c, is given by $1 - Rv/(Y_{A^+\to C} + RY_{C^+\to C}) = 0$ in the right-hand side of Eq. (4). On the other hand, in the present model, the normalized effective sputtering yield is found to start to decrease gradually at another critical ratio, $R_{c'}$, which is given by $\partial Y_{eff}(R)/\partial R = 0$. These erosion behavior are mainly coming from the change of the surface concentration due to the deposited carbon represented by the second bracket in the right-hand side in Eq. (4).

For argon plasmas, the normalized effective sputtering yield is monotonically decreasing with R as shown in Fig. 1(b). The transition from enhanced erosion and suppressed erosion shown in Fig. 1(a) for hydrogen plasmas cannot be observed. When the sputtering yield of molybdenum by argon is much greater than that by carbon, then the first bracket in the right-hand side of Eq. (4) $1 + R \cdot Y_{\mathrm{C}^+\to\mathrm{Mo}}/Y_{\mathrm{A}^+\to\mathrm{Mo}}$ is almost unity. Therefore, we see only the reduction of the effective sputtering yield represented by $1 - Rv/(Y_{\mathrm{A}^+\to\mathrm{C}} + RY_{\mathrm{C}^+\to\mathrm{C}})$ in the right-hand side of Eq. (4).

3. Experimental set-up

The water-cooled molybdenum target plate to be bombarded by argon plasmas was installed at the end of the plasma column in a linear divertor plasma simulator, NAGDIS-I (Nagoya University Divertor Simulator) [7], as shown in the inset of Fig. 2. The molybdenum target plate was negatively biased by a dc power supply to control the incident ion energy. The incident ion energy is determined by the difference between the target potential and plasma potential measured with a fast scanning Langmiur probe. Methane was introduced through the inlet located at 65 cm away from the target plate as a source of the carbon impurity. The erosion behavior of molybdenum was monitored with the spectroscopic method [7] by measuring the intensity of the MoI spectral line (379.8 nm), which is proportional to the sputtered molybdenum neutral flux when plasma parameters (electron density and temperature) are constant. At the same time, ArI (419.8 nm) was measured to monitor plasma parameters.

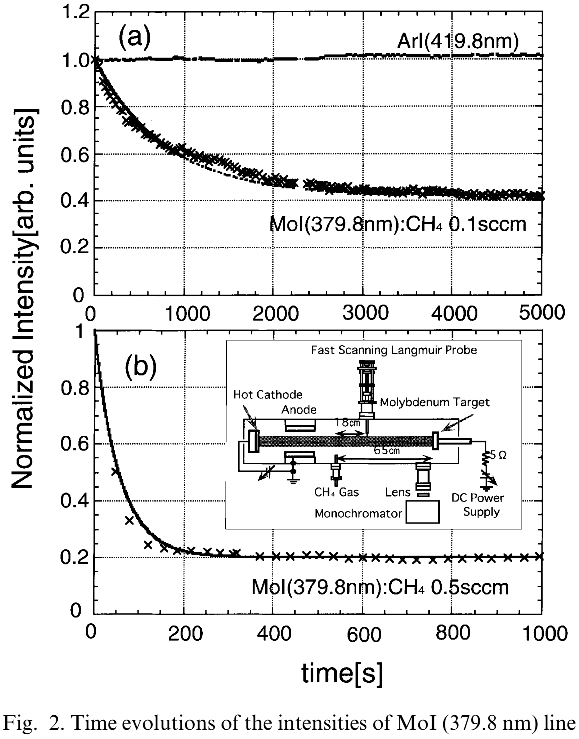

Fig. 2. Time evolutions of the intensities of MoI (379.8 nm) line and ArI (419.8 nm) at a different gas flow rate of the methane gas: (a) 0.1 sccm; (b) 0.5 sccm ('sccm' means 'standard cubic centimeter per minute' and 1 sccm corresponds to 2.7×10^{18} s^{-1}). The inset of (b) shows the schematic of experimental setup.

4. Results and discussion

The MoI line emission intensity is shown as a function of irradiated time in Fig. 2, compared with the intensity of the ArI line. The plasma density was 1.0×10^{17} m^{-3} and the electron temperature was 4.0 eV measured with the fast scanning probe. At $t = 0$ s, methane was introduced into the host argon plasma. The intensity of ArI is found to be constant with time, meaning little change of plasmas parameters, which guarantees that emission intensity of MoI line is proportional to the molybdenum neutral flux from the target plate. On the other hand, it is clearly observed that the intensity of MoI line decrease with time to a steady-state level. These experimental results indicate that the effective sputtering yield of molybdenum becomes smaller than that in pure argon plasma. Moreover, the decay time of the time evolution of MoI line emission is found to be smaller with an increase in the gas flow rate of methane, which can be predicted by Eqs. (2) and (3) because the decay time is given by $[\Gamma_{\mathrm{A}^+}(\sigma_{\mathrm{A}^+\to\mathrm{C}} + R\sigma_{\mathrm{C}^+\to\mathrm{C}})]^{-1}$. The fitting curves in Fig. 2 are obtained from Eq. (3) with the argon ion flux $\sim 1.8 \times 10^{19}$ m^{-2} s^{-1} and the bombarded energy $\sim$100 eV. The carbon flux is assumed to be 2.0×10^{16} m^{-2} s^{-1} for the gas flow rate of methane $F \sim 0.1$ sccm in Fig. 2(a) and 7.8×10^{16} m^{-2} s^{-1} for $F \sim 0.5$ sccm in Fig. 2(b). The calculated results can reproduce the experimental ones well.

Fig. 3 shows the steady-state intensities of the MoI emission line as a function of the gas flow rate of methane, F. The steady-state intensities are corre-

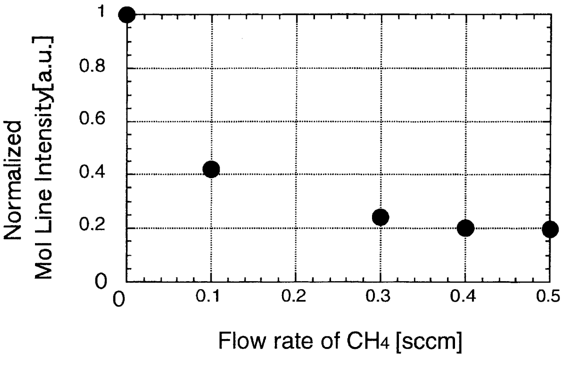

Fig. 3. Dependence of normalized MoI line intensities as a function of the flow rate of methane.

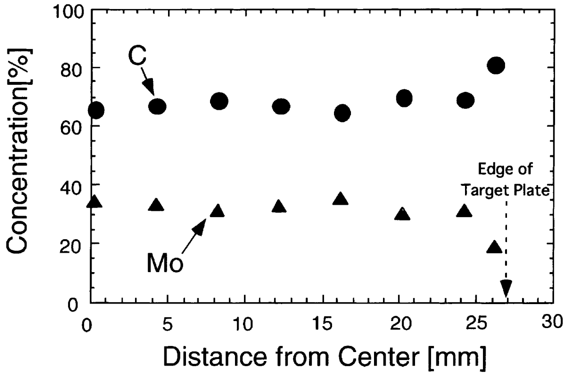

Fig. 4. Profile of the concentration of carbon on the molybdenum surface after the plasma bombardment corresponding to Fig. 2(b).

sponding to the effective sputtering yields determined by Eq. (4). It is shown that the intensities are monotonically decreasing with an increase in *F*, which agrees with Fig. 1(b) for argon plasmas. After the bombardment of argon–carbon mixing plasmas to the molybdenum target plate corresponding to Fig. 2(b), we have analyzed the plasma-bombarded surface with an energy dispersion type X-ray spectroscopy. Fig. 4 shows the profile of the surface concentration of carbon on the Mo surface. It has been found that about 70% of the Mo surface was covered with carbon impurities, which is in reasonable agreement with the experimental data in Figs. 2 and 3. These experimental results clearly indicate that the deposition of condensible impurities can suppress the host material erosion.

In order to compare experimental data with model calculations more quantitatively, it is necessary to know the exact value of the carbon flux to the target plate. However, there is no experimental data for the carbon flux. The carbon flux is determined by the atomic-processes (ionization and dissociation) starting from the methane gas and the transport in plasmas. In order to discuss the value of the carbon flux to the Mo surface, we have investigated the break-up processes of methane in plasmas and its transport by three-dimensional Monte-Carlo simulation code [8] by taking experimental conditions into account. Fig. 5 shows the dependence of the ratio between the numbers of the introducing methane and carbon species entering the target plate on plasma density. It is found that the 0.5% methane can reach the target plate as a carbon when the plasma density is 1.0×10^{17} m^{-3} and the ratio becomes larger with the plasma density. From this result, we can estimate the carbon flux to be 2.3×10^{16} $\mathrm{m}^{-2}\ \mathrm{s}^{-1}$ at the gas flow rate of methane $F = 0.1$ sccm, which is in reasonable agreement with the carbon flux used in the fitting of Fig. 2(a).

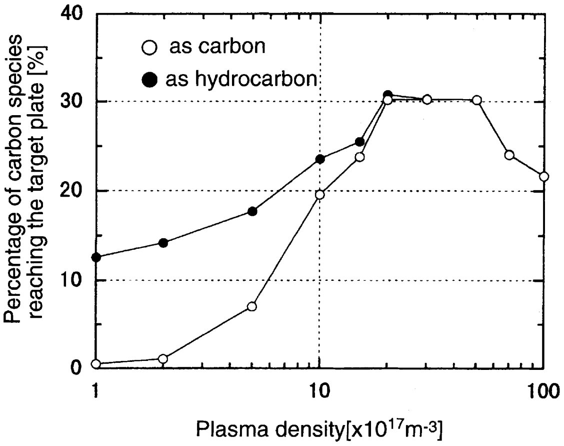

Fig. 5. Calculated results by three-dimensional Monte-Carlo simulation code. Open circles (closed circles) mean the ratio of the carbon (hydro-carbon) flux to the target plate to introducing methane gas flux.

5. Conclusion

The reduction of effective sputtering yields due to the surface coverage with carbon impurities has been clearly observed in the experiments where molybdenum was bombarded with argon plasmas into which methane was introduced. A new formula has been deduced by taking the change of the surface composition with the impurity deposition into account, which can explain the experimental results well.

Acknowledgements

One of authors (N.O) would like to thank Dr M. Kojima for using three-dimensional Monte-Carlo simulation code and Professor K. Morita for very fruitful discussion for the numerical modeling.

References

[1] Y. Hirooka, J. Nucl. Mater. 258–263 (1998) 1045.
[2] D. Naujoks, W. Eckstein, J. Nucl. Mater. 220–222 (1995) 993.
[3] P. Wienhold et al., J. Nucl. Mater. 266–269 (1999) 986.
[4] S. Takamura, K. Yamamoto, K. Morita, Jpn. J. Appl. Phys. 37 (1998) 266.
[5] N. Matsunami et al., Atom. Data Nucl. Data Tables 1 (1984) 1.
[6] W. Eckstein et al., Max-Planck-Institute Report#IPP9/82, 1993.
[7] M. Kojima, S. Takamura, J. Nucl. Mater. 220–222 (1995) 1107.
[8] M. Kojima, S. Takamura, J. Nucl. Mater. 241–243 (1998) 1248.